Effect of Connected and Automated Vehicles on Disturbance Suppression in Mixed Traffic Flow: Spatial Distribution and Stability

Feng Yue[1], Rui Zhang[1,*], Yuelei Zhang[2]
[1]School of Automobile and Transportation, Tianjin University of Technology and Education, South Dagu St. 1310, Tianjin, 300222, China
[2]Jiujiang Polytechnic University of Science and Technology, Gongqing St. 1, Jiujiang 332020, China
0721231017@tute.edu.cn; [*]zhangrui318@163.com; zyl3836@sina.com

***Abstract*—With the progressive integration of connected and automated vehicles (CAVs) into existing transportation systems, the characteristics of mixed traffic flow comprising CAVs and human-driven vehicles (HDVs) undergo a profound transformation. However, the combined effects of the CAV penetration rate and spatial distribution on mixed-flow performance have not been thoroughly investigated. To address this gap, this study develops a generalised modelling framework for mixed traffic, in which separate car-following models are specified for HDVs and CAVs, and microscopic traffic simulations are carried out under traffic oscillation scenarios. The results demonstrate that increasing the penetration rate of the CAV markedly enhances the operational performance of the mixed flow. On this basis, the impact of CAV spatial distribution strategies is examined. Numerical experiments reveal that platoon-based arrangements of CAVs are not globally optimal; notably, when HDV stability is poor, the performance gains of platooning are minimal, while a uniform distribution of CAVs yields superior suppression of traffic disturbances. These findings indicate that, in realistic mixed traffic environments, CAV deployment strategies should go beyond traditional platooning and explore more diversified spatial distribution patterns to optimise traffic flow performance.**

***Index Terms*—Connected and automated vehicles; Mixed traffic flow; Vehicle dynamics.**

I. INTRODUCTION

With the rapid advancement of high-precision perception and low-latency communication technologies, connected and automated vehicles (CAVs) are gradually entering real-world deployment. By combining advanced sensing, communication, and automated driving functions, CAVs can markedly shorten reaction times, achieve beyond line-of-sight awareness, and accurately perceive surrounding traffic [1]. Yet, in practice, they coexist with human-driven vehicles (HDVs) at varying penetration rates and exhibit heterogeneous spatial distributions, introducing significant uncertainties. Against the backdrop of the vision of "zero-accident", a deeper understanding of the behaviour of CAVs in mixed traffic is vital to inform large-scale deployment strategies.

Manuscript received 3 April, 2025; accepted 7 August, 2025.

A. Impact of Mixed Traffic Flow

Adaptive cruise control (ACC) and cooperative ACC (CACC) have garnered significant academic and industrial interest. A vehicle-road collaborative control framework was first proposed to exploit the vehicle-to-vehicle (V2V) and vehicle-to-infrastructure (V2I) communications [2]. Subsequent studies have modelled the impact of ACC on traffic flow: Dong, Wang, Chen, Gao, and Luo [3] showed that ACC markedly reduces speed oscillations and enhances the stability of the strings at penetration rates. Xiao, Wang, Schakel, and van Arem [4] found that ACC failures in merging bottlenecks intensify local congestion and emissions. A connected vehicle management strategy was proposed to optimise CAV penetration and vehicle-road logic to ensure robust mixed-flow stability [5]. Furthermore, an "Eco-CACC" framework, combining lane change control with soft speed constraints, was introduced to suppress acceleration-deceleration waves while improving efficiency and energy use [6]. ACC was reported to reduce the total delay by 7 % and delay congestion onset [7] and proper ACC tuning can smooth lane change disturbances and limit congestion spread [8]. More recent advances include time-varying spacing ACC, virtual CAV testing, platoon CACC, etc.

B. Formation and Control of Multiple CAVs

In multi-vehicle platooning, multiple CAVs travel in a coordinated formation, a concept pioneered by the PATH project in the 1980s and later explored by initiatives such as GCDC [9], SARTRE [10], and Energy-ITS [11]. Both theoretical analyses and experiments confirm that platooning can significantly enhance road capacity and safety. Du, Huang, Li, and Zhang [12] extended fundamental diagram models with platoon strength and varying delays to assess mixed flow stability. Zheng *et al.* [13] used real-vehicle tests and microsimulation for mixed CAV traffic. Ren, Zhao, Li, and Fu [14] quantitatively evaluated heterogeneous platoons on highways.

However, in practice, CAVs are often sparse and randomly distributed at low penetration rates. Forming a contiguous platoon requires vehicle joining, departure, lane change, and

splitting manoeuvres, which can inadvertently cause congestion [15]. These findings suggest the need to reconsider whether contiguous platooning is the optimal CAV arrangement in mixed traffic. Since CAVs need not travel continuously, alternative patterns, such as uniform spacing or random dispersion (see Fig. 1), may be more effective. From this perspective, Li, Wang, and Zheng [16] proposed diversified cooperative formations beyond contiguous platoons, and subsequent theoretical and simulation studies have confirmed that optimised spatial distributions can enhance mixed-flow performance.

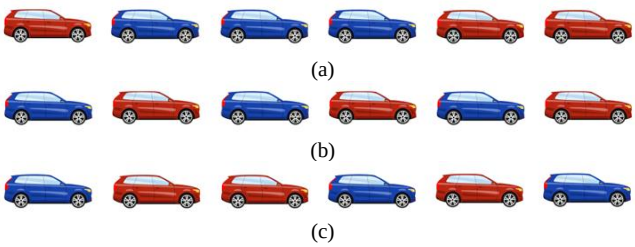

(a)

(b)

(c)

Fig. 1. Examples of three possible CAV deployment patterns in mixed traffic flow. Blue vehicles denote CAVs, and red vehicles denote (human-driven vehicles, HDVs): (a) Platoon formation; (b) Uniform formation; (c) Random formation.

This study focusses on the role of CAV deployment patterns in enhancing traffic performance and in identifying the optimal CAV arrangement in mixed traffic environments. Specifically, we define separate car-following models for CAVs and HDVs within a unified mixed traffic framework, systematically analyse, through theoretical stability analysis and numerical simulation, the impacts of CAV penetration rate and spatial distribution on traffic performance.

Through stability analysis, the optimal spatial distribution of CAVs is not limited to platooning; Under poor HDV string stability conditions, a uniform distribution often outperforms a platoon-based arrangement.

This paper makes two primary contributions:

1. It provides a comprehensive evaluation of how the CAV penetration rate and spatial distribution each contribute to traffic flow improvement;
2. It demonstrates that the optimal CAV deployment pattern depends critically on the string stability of HDVs - when HDV string stability is poor, platooning may not be the best choice.

The remainder of this paper is organised as follows. Section II introduces our general mixed traffic modelling framework and defines the HDV and CAV car-following models. Section III presents the HDV stability analysis and shows that increasing the CAV penetration rate improves mixed flow performance. Section IV describes spatial-distribution simulation experiments and stability metrics. Section V concludes the paper.

II. MIXED TRAFFIC SYSTEM MODELLING

A. *Ring-Road Traffic Flow System*

This paper focusses on the longitudinal dynamics of mixed traffic flow on a closed ring road, where human-driven vehicles (HDVs) and connected and automated vehicles (CAVs) are randomly interspersed (lane-changing behaviour is not considered). As shown in Fig. 2, this periodic closed environment represents an infinitely long traffic stream. Many previous studies have employed closed ring-road systems to emulate continuous roadway segments, highlighting their theoretical advantages in traffic flow simulation, such as enabling precise calibration of model parameters, achieving perfect control of average traffic density, and corresponding directly to infinite, periodic traffic dynamics. Moreover, by applying a localised disturbance, one can observe how the system evolves according to its inherent characteristics and directly visualise the impact of the initial perturbation on the eventual steady state, thereby eliminating interference from boundary inflow or outflow effects. Vehicles travel tangentially along the ring. For conventional vehicles, standard car-following models relate the acceleration of a vehicle to its own speed, the spacing to the preceding vehicle, and their relative velocity, while accounting for the delay in driver reaction time. This relationship can be expressed as in (1)

$$\dot{v}_n\left(t+\tau_{\mathrm{R}}\right)=f\left(v_n\left(t\right),s_n\left(t\right),\Delta v_n\left(t\right)\right), \tag{1}$$

where τ_{R} denotes the human driver's reaction time, $f(.)$ represents the specific functional form of the car-following model, $v_n(t), s_n(t), \Delta v_n(t)$ denote the vehicle's speed, the spacing to the preceding vehicle, and the relative velocity, respectively.

For CAVs, emerging perception and communication technologies enable real-time acquisition of surrounding vehicle state information and faster responses to changes in traffic dynamics. Consequently, leveraging these capabilities, the model can be generalised to the form shown in (2)

$$\begin{aligned}\dot{v}_n\left(t+\tau_A\right)=&f\left(v_n\left(t\right),s_n\left(t\right),\Delta v_n\left(t\right)\right)+\\&+\Gamma\left(I_k\right)\left(t+\tau_C\right),k\in V,\end{aligned} \tag{2}$$

where τ_A denotes the reaction time of a connected and automated vehicle, which is shorter than the human driver reaction time τ_{R}, I_k represents the influence of the k^{th} leading vehicle's acceleration on the subject vehicle, τ_C denotes the V2V communication delay, and V is the set of CAVs within the communication range from which the subject vehicle can obtain state information.

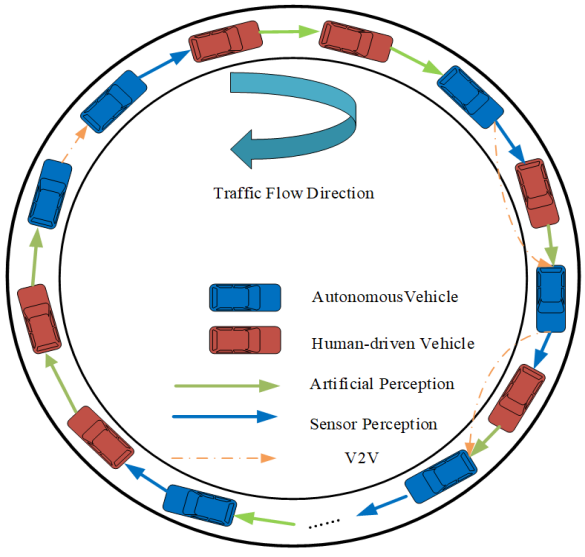

Fig. 2. Mixed ring-road traffic system.

B. Human-Driven Vehicle Model

Car-following models have been extensively studied in the literature, with various formulations proposed, such as the intelligent driver model (IDM), the optimal velocity model (OVM), and the full velocity difference (FVD) model. Compared to other approaches, IDM offers greater realism in capturing driver behaviour and effectively reflects diverse characteristics of traffic congestion. Therefore, this paper adopts the IDM to describe HDV behaviour, whose mathematical expressions are given in (3) and (4):

$$\dot{v} = a\left[1-\left(\frac{v}{v_0}\right)^{\delta}-\left(\frac{s^*(v,\Delta v)}{s}\right)^2\right], \tag{3}$$

$$s^*(v,\Delta v) = s_0 + max\left(0, vT + \frac{v\Delta v}{2\sqrt{ab}}\right), \tag{4}$$

where a denotes the maximum acceleration, b is the comfortable deceleration, v_0 is the desired speed, s_0 is the minimum spacing, δ\delta is the acceleration exponent, and T is the safe time headway. The typical values of the IDM parameters are shown in Table I.

TABLE I. PARAMETERS OF THE CAR-FOLLOWING MODELS

Parameters	HDV	CAV
Desired velocity (m/s)	14.5	14.5
Jam gap (m)	2	2
Maximum acceleration (m/s^2)	1.5	1.5
Minimum deceleration (m/s^2)	2	2
Safety time Headway (s)	1.5	0.6
Delay (s)	0.6	0.1
K_p		0.45
K_d		0.25

The mixed traffic system, composed of connected and automated vehicles (CAVs) and human-driven vehicles (HDVs), exhibits complex dynamical behaviour due to intervehicle interactions and driver reaction delays. Therefore, the IDM is first linearised on its equilibrium state to facilitate subsequent analysis.

In equilibrium, all vehicles travel at the same speed v, maintain a spacing s, and have $\Delta v = 0$; the equilibrium state satisfies

$$\dot{v} = 0 \Rightarrow 1-\left(\frac{v}{v_0}\right)^{\delta}-\left(\frac{s^*(v,0)}{s}\right)^2 = 0, \tag{5}$$

where $s^*(v,0) = s_0 + vT$, at equilibrium, the spacing s must satisfy

$$\left(\frac{s_0+vT}{s}\right)^2 = 1-\left(\frac{v}{v_0}\right)^{\delta}. \tag{6}$$

When linearising near the equilibrium state, it is necessary to account for small perturbations in vehicle position and velocity. To analyse string stability, we consider the linearised IDM model around its equilibrium. Let s_n, v_n and a denote the position, velocity, and acceleration of vehicle n, respectively, and let vehicle n-1 be its immediate predecessor. The IDM model can be described as

$$f(s_n, v_n, \Delta v_n) = a\left[1-\left(\frac{v_n}{v_0}\right)^{\delta}-\left(\frac{s^*(v_n,\Delta v_n)}{s_n}\right)^2\right]. \tag{7}$$

Linearise the function $f(s_n, v_n, \Delta v_n)$ at the equilibrium state $(s, v, 0)$

$$\dot{v}_n \approx f(s,v,0) + \left.\frac{\partial f}{\partial s}\right|_{\text{eq}}\tilde{s}_n + \left.\frac{\partial f}{\partial v}\right|_{\text{eq}}\tilde{v}_n + \left.\frac{\partial f}{\partial \Delta v}\right|_{\text{eq}}\Delta v_n. \tag{8}$$

Since at the equilibrium point $f(s,v,0) = 0$, it follows

$$\dot{\tilde{v}}_n = \alpha\tilde{s}_n + \beta\tilde{v}_n + \gamma\Delta v_n, \tag{9}$$

where $\alpha = \left.\frac{\partial f}{\partial s}\right|_{\text{eq}}, \beta = \left.\frac{\partial f}{\partial v}\right|_{\text{eq}}, \gamma = \left.\frac{\partial f}{\partial \Delta v}\right|_{\text{eq}}$.

$$\frac{\partial f}{\partial s} = a\times\left(\frac{\partial}{\partial s}\left(\frac{\left(s^*\right)^2}{s^2}\right)\right) = 2a\frac{\left(s^*\right)^2}{s^3}. \tag{10}$$

At the equilibrium point $s^* = s_0 + vT$, and $\frac{s^*}{s} = \sqrt{1-(v/v_0)^{\delta}}$. Here, we directly denote them by $s^*$and s

$$\frac{\partial f}{\partial v} = a\left[-\delta\frac{v^{\delta-1}}{v_0^{\delta}} - \frac{2s^*}{s^2}\cdot\frac{\partial s^*}{\partial v}\right]. \tag{11}$$

Near the equilibrium point $\Delta v = 0$, since we have $s^* = s_0 + vT$,

$$\frac{\partial s^*}{\partial v} = T. \tag{12}$$

Hence:

$$\frac{\partial f}{\partial v} = a\left[-\delta\frac{v^{\delta-1}}{v_0^{\delta}} - \frac{2s^*}{s^2}T\right], \tag{13}$$

$$\frac{\partial f}{\partial \Delta v} = -a\frac{2s^*}{s^2}\cdot\frac{v}{2\sqrt{ab}} = -a\frac{s^*v}{s^2\sqrt{ab}}. \tag{14}$$

Now obtain the linearised model

$$\dot{\tilde{v}}_n = \alpha\tilde{s}_n + \beta\tilde{v}_n + \gamma\Delta v_n, \tag{15}$$

where:

$$\alpha = 2a\frac{\left(s^*\right)^2}{s^3}, \tag{16}$$

$$\beta = a\left[-\delta\frac{v^{\delta-1}}{v_0^{\delta}} - \frac{2s^*T}{s^2}\right], \tag{17}$$

$$\gamma = -a\frac{s^*v}{s^2\sqrt{ab}}. \tag{18}$$

C. Car-Following Model

As discussed above, connected and automated vehicles (CAVs) feature shorter reaction times and access to

additional vehicle-state information, allowing feedforward effects on the ego-vehicle dynamics to be modelled via the velocity difference with the preceding vehicle. In this work, we adopt the PD-control-based CAV car-following model proposed by the PATH Laboratory at the University of California, Berkeley. Its structure is described by:

$$\begin{cases} v = v_{\text{pre}} + k_{\text{p}} e + k_{\text{d}} \dot{e}, \\ e = h - s_0 - L - vT, \\ \dot{e} = v_l - v - aT, \end{cases} \tag{19}$$

where v denotes the vehicle speed, v_{pre} denotes the speed at the previous time step, k_{d} and k_{p} are the proportional and derivative control gains, s_0 is the minimum safety gap, h is the current headway, T is the safe time headway, L is the vehicle length, e is the spacing error, and v_l is the speed of the lead vehicle. The model parameters are listed in Table I.

III. Synergistic Effects of HDVs and CAVs

In this section, first we perform a stability analysis of the IDM model to derive the critical condition required to maintain string stability. Then design and conduct microscopic simulations of mixed traffic oscillations to explore how the CAV penetration rate affects traffic flow performance.

A. Stability Analysis of IDM Model

In this section, periodic boundary conditions are assumed, and the stability of the IDM model described in (3) and (4) is analysed. Under equilibrium and stable conditions, the following equation is solved as

$$f(s, v, 0) = 0, \tag{20}$$

where we consider the transfer function. Assuming that the speed of the lead vehicle is subject to a sinusoidal disturbance, the transfer function for the n[th] vehicle is defined as

$$G_n(\omega) = \frac{\hat{v}_n(\omega)}{\hat{v}_0(\omega)}. \tag{21}$$

For a linear chain system, the transfer function between adjacent vehicles is typically considered. If the transfer function gain between adjacent vehicles does not exceed unity, then the entire platoon is string stable

$$\left|G_n(\omega)\right| \le 1. \tag{22}$$

Considering two adjacent vehicles, let the lead vehicle speed disturbance be $\tilde{v}_{n-1}(t) = \hat{v}_{n-1} e^{i\omega t}$ and the following vehicle disturbance be $\tilde{v}_n(t) = \hat{v}_n e^{i\omega t}$. According to the linearised equation, it yields:

$$i\omega \tilde{s}_n = \tilde{v}_{n-1} - \tilde{v}_n, \tag{23}$$

$$\dot{\tilde{v}}_n = \alpha \tilde{s}_n + \beta \tilde{v}_n + \gamma\left(\tilde{v}_{n-1} - \tilde{v}_n\right). \tag{24}$$

Simplifying (24), we obtain

$$\tilde{v}_n\left(i\omega - \beta + \frac{\alpha}{i\omega} + \gamma\right) = \tilde{v}_{n-1}\left(\frac{\alpha}{i\omega} + \gamma\right). \tag{25}$$

Therefore, the transfer function is as follows

$$G_n(\omega) = \frac{\alpha + \gamma i\omega}{\alpha - \omega^2 + i\omega(\gamma - \beta)}. \tag{26}$$

The condition for string stability is that, for all real ω, $|G_n(\omega)| \le 1$. Compute the squared magnitude as

$$G_n(\omega) = \frac{(\alpha)^2 + (\gamma\omega)^2}{\left(\alpha - \omega^2\right)^2 + \omega^2(\gamma - \beta)^2}. \tag{27}$$

Therefore, the condition for string stability is

$$(\alpha)^2 + (\gamma\omega)^2 \le \left(\alpha - \omega^2\right)^2 + \omega^2(\gamma - \beta)^2. \tag{28}$$

For all ω the following holds, it derives

$$0 \le \omega^4 + \omega^2\left[-2\alpha + \beta^2 - 2\gamma\beta\right]. \tag{29}$$

Letting $\omega^2 = \eta$ for any $\eta \ge 0$, the necessary and sufficient condition for string stability is

$$\beta^2 - 2\gamma\beta - 2\alpha \ge 0, \tag{30}$$

where the linear stability index ξ is defined as

$$\xi = \beta^2 - 2\gamma\beta - 2\alpha. \tag{31}$$

Therefore, the necessary and sufficient condition for an HDV to maintain stability is $\xi \ge 0$.

B. Numerical Simulation

A stability perturbation experiment was performed by shifting the position of vehicle 1 rearward by 5 m at a specified instant to introduce a disturbance. The simulated platoon comprised 100 vehicles, sequentially numbered from 1 to 100, with the proportions and spatial locations of the CAVs and HDVs assigned randomly according to the specified CAV penetration rate. Vehicles maintained a uniform constant speed throughout the simulation.

All tests were conducted under periodic boundary conditions on a closed ring road without entry or exit, having an initial circumference of L = 3600 m. The HDV and CAV followed the models described in Section II, with parameter values given in Table I. The vehicle length was set at 4 m and both HDVs and CAVs were randomly distributed along the ring. The equilibrium speed was 14.5 m/s, the simulation duration was 2000 s, and the integration time step was 0.1 s. CAV penetration rates of P = [0, 0.2, 0.4, 0.6, 0.8, 1.0] were examined.

Figure 3 illustrates the spatio-temporal velocity evolution of a 100-vehicle platoon at an equilibrium speed of 14.5 m/s after a single abrupt deceleration disturbance, for varying CAV penetration rates. Under 0 % CAV (Fig. 3(a)), the traffic flow is unstable: the platoon lacks sufficient internal damping and fails to satisfy the stability criterion.

Consequently, the disturbance is amplified into disturbance energy and is instantaneously absorbed. Overall, each 20 percentage points increase in CAV penetration increases the minimum speed by 1–2 m/s and reduces the propagation distance by 15–20 vehicles; once penetration exceeds approximately 60 %, the platoon exhibits pronounced overdamped behaviour, absorbing abrupt perturbations within a very short distance. In summary, Fig. 3 shows that as penetration increases, congestion is progressively suppressed and speed fluctuations diminish, such that at P = 0.8 and 1.0, congestion nearly disappears and speed variations become negligible. These results confirm that the lower response latency of CAVs and V2V communication can effectively suppress traffic waves.

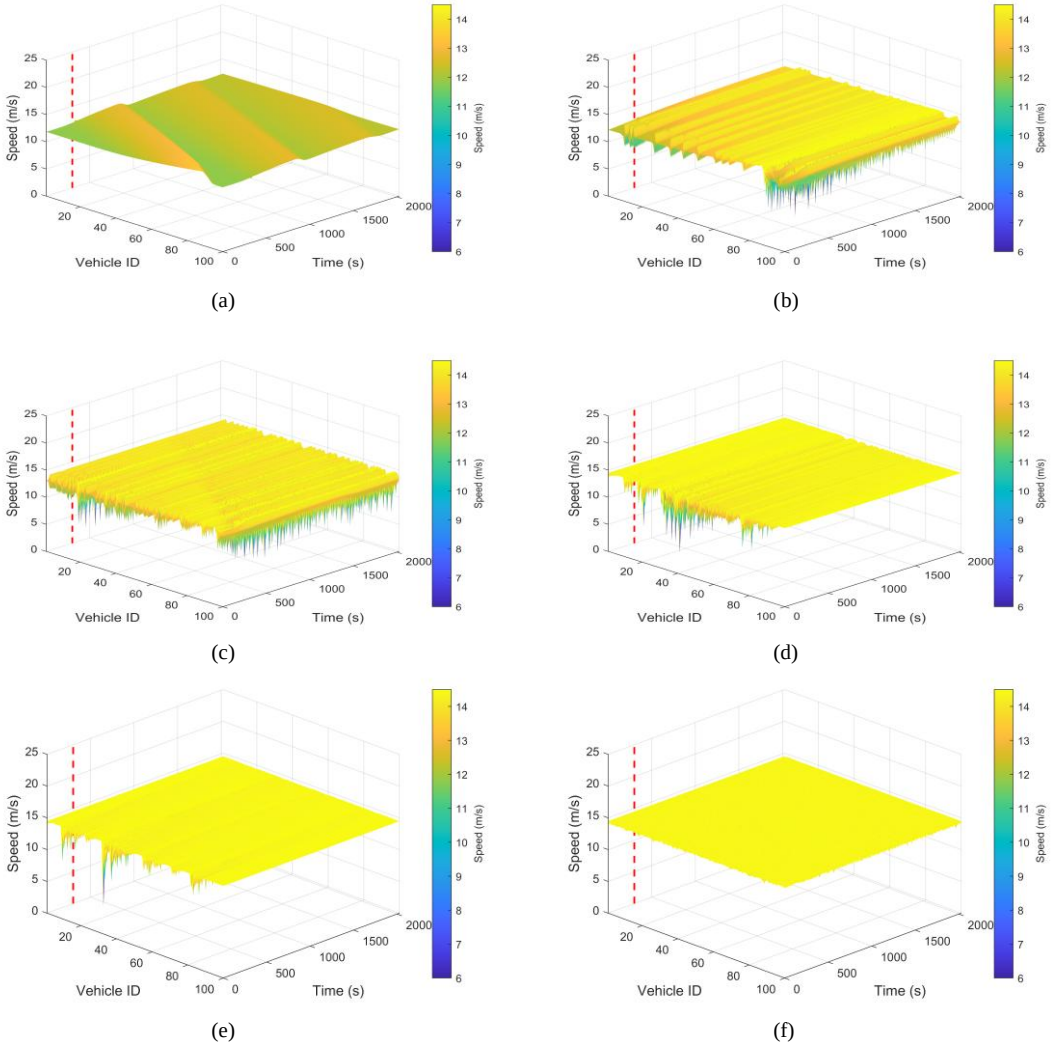

Fig. 3. Spatiotemporal evolution of the velocity for penetration rates P = [0, 0.2, 0.4, 0.6, 0.8, 1.0]: (a) CAV penetration rate P = 0; (b) CAV penetration rate P = 0.2; (c) CAV penetration rate P = 0.4; (d) CAV penetration rate P = 0.6; (e) CAV penetration rate P = 0.8; (f) CAV penetration rate P = 1.0.

IV. SPATIAL DISTRIBUTION OF CAVS

Currently, the conditions for large-scale field testing of CAVs remain immature. Therefore, simulation testing is a necessary approach to evaluate the performance of CAVs in mixed traffic flows. In this section, we conduct a simulation experiment to investigate different spatial distributions of CAVs on a ring road, with the aim of identifying the optimal deployment under varying traffic conditions.

A. Uniform Distribution and Platoon Distribution

The spatial distribution of CAVs is a critical factor affecting mixed-flow performance. Two typical patterns are the uniform distribution and the platoon distribution. Figure 4 illustrates an example in which a mixed platoon of 40 vehicles, with a CAV penetration rate of 20 % (8 CAVs), is organised according to three spatial patterns: uniform distribution, platoon distribution, and random distribution.

B. Simulation Experiment Design and Analysis

For the uniform distribution, we set the CAV positions as S = {3, 8, 13, 18, 23, 28, 33, 38}, while for the platoon distribution we set S = {17, 18, 19, 20, 21, 22, 23, 24}. We also consider a random distribution with S = {5, 18, 19, 31, 32, 33, 38, 40}. The nonlinear IDM is used to model HDV car-following behaviour. To reflect realistic traffic conditions, parameter values are those listed in Table I. We examine a scenario in which a single vehicle experiences a sudden, rapid disturbance - typical during lane changes or merging. Specifically, traffic starts from equilibrium, and at t = 50 s, one vehicle decelerates at -3 m/s² for 1.5 s.

Figure 5 shows the speed trajectory and the residual speed of vehicle 15 following the disturbance. In each subplot, the blue and grey curves represent CAV and HDV speeds, respectively, and the red dashed line marks the disturbance onset. In Fig. 5(a), the CAVs form a platoon; in Fig. 5(b), they

are uniformly distributed, and in Fig. 5(c), they are randomly distributed.

Combining the two sets of plots makes it clear that, among the three CAV distribution strategies, disturbance suppression follows a distribution produces a pronounced trough that spans almost the entire 40-vehicle platoon and propagates rearward, only gradually decaying; within the eight-vehicle CAV subplatoon the amplitude drops sharply, yet residual oscillations still penetrate deep into the HDV tail. By contrast, the uniform distribution immediately truncates the wave at the next CAV node - only vehicles 13 and 14 exhibit slight speed dips, and downstream of vehicle 18 the velocity field is essentially restored to flatness. The random distribution displays an intermediate behaviour: the speed trough caused by the perturbation passes unimpeded through the first gap until it meets the next randomly placed CAV, resulting in staggered, irregular attenuation; some downstream HDVs experience a longer delay before encountering the next CAV "damper", producing patchy infiltration, although the overall decay is still faster than in the platoon case.

The speed-residual heat maps further confirm this ranking. In the platoon configuration, a continuous diagonal band of negative residuals extends from vehicle 15 to the platoon tail, only dissipating near the end of the simulation. In the uniform-spacing scenario, that diagonal band is confined to two or three vehicles and vanishes almost immediately after vehicle 18, leaving only green (near-zero change) elsewhere. The random layout again exhibits a mixed pattern: whenever the disturbance encounters a stretch of HDVs without intervening CAVs, multiple short diagonals appear, but each blue band is cut off at the next CAV location, so residual oscillations never fuse into a long, deep wave as in the platoon distribution.

Figure 6 illustrates the spatiotemporal trajectory plots for the platoon and uniform CAV distributions. Under platoon distribution, CAVs exhibit very tight parallel trajectories. These trajectories quickly revert to linearity within the platoon, but leave a slight velocity curvature that propagates rearward through the following HDVs. In contrast, uniformly distributed CAVs form multiple interleaved lines that absorb disturbance; after each brief deviation, the trajectories immediately return to a neat, parallel ascent. Therefore, although the platoon distribution concentrates the damping locally, the uniform CAV distribution more effectively prevents the propagation of disturbances throughout the traffic stream.

In summary, uniformly distributed CAVs provide the most robust and repeatable barrier to disturbance propagation; platoon distribution, while concentrating damping capability locally, allows residual oscillations to persist for longer; and random distribution performs intermediately, with its effectiveness highly sensitive to the actual spatial arrangement.

Conduct numerical simulations through three sets of experiments to investigate whether HDV stability influences the effectiveness of CAVs in improving mixed traffic flow performance. The stability index is shown in Table II.

TABLE II. LINEAR STABILITY INDICATORS.

	α	β	γ	ξ	**Stability**
(a)	0.186	-1.32	-0.37	0.351	Strong
(b)	0.103	-0.88	-0.35	0.041	Weak
(c)	0.201	-0.42	-0.24	-0.382	Instability

When examining the three-dimensional velocity response surfaces as HDV instability increases, a clear pattern emerges (Fig. 7). When HDVs are inherently string stable, deploying CAVs in a platoon yields the most pronounced initial attenuation of the shock introduced by vehicle 18 at t = 50 s: the disturbance is almost entirely absorbed within the platoon, with only minimal residuals propagating upstream. Under marginal (weak) HDV stability, the platoon still achieves a significant reduction in wave amplitude, but slight residual growth is observed within the HDV segments. In contrast, a uniform CAV layout repeatedly intercepts and attenuates the perturbation, producing a smoother, monotonic decay. Crucially, when HDVs are fully unstable, only the uniform CAV distribution prevents exponential amplification of the disturbance. Thus, for highly stable or weakly stable traffic flows, platooning effectively concentrates damping capacity; however, in inherently unstable flows, uniform CAV deployment is required to suppress disturbances before they can grow.

Note that, due to long driver reaction times and limited perceptual capabilities, most HDVs typically exhibit poor string stability. These findings suggest that in mixed traffic environments, platooning can constrain the potential of CAVs to enhance real-world traffic efficiency compared to other deployment strategies. When HDV string stability is poor, uniformly distributing CAVs helps fully leverage their ability to suppress traffic perturbations and improve flow stability; conversely, when human drivers demonstrate strong string stability performance, organising CAVs into platoons may prove to be the superior choice.

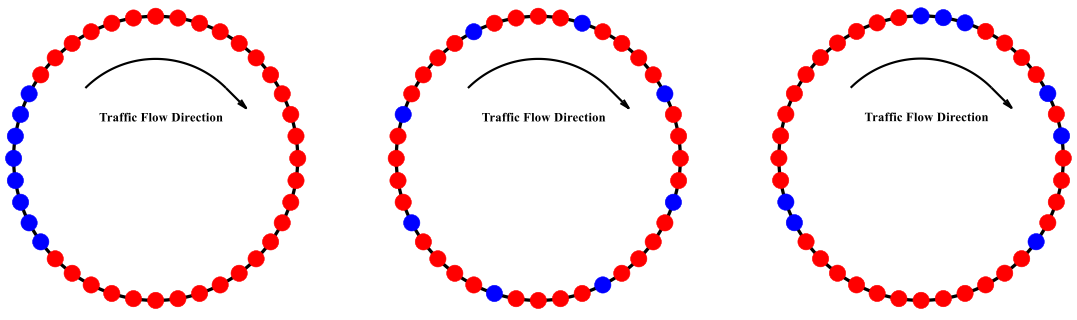

(a) (b) (c)

Fig. 4. Spatial distribution of CAV: (a) Platoon distribution; (b) Uniform distribution; (c) Random distribution.

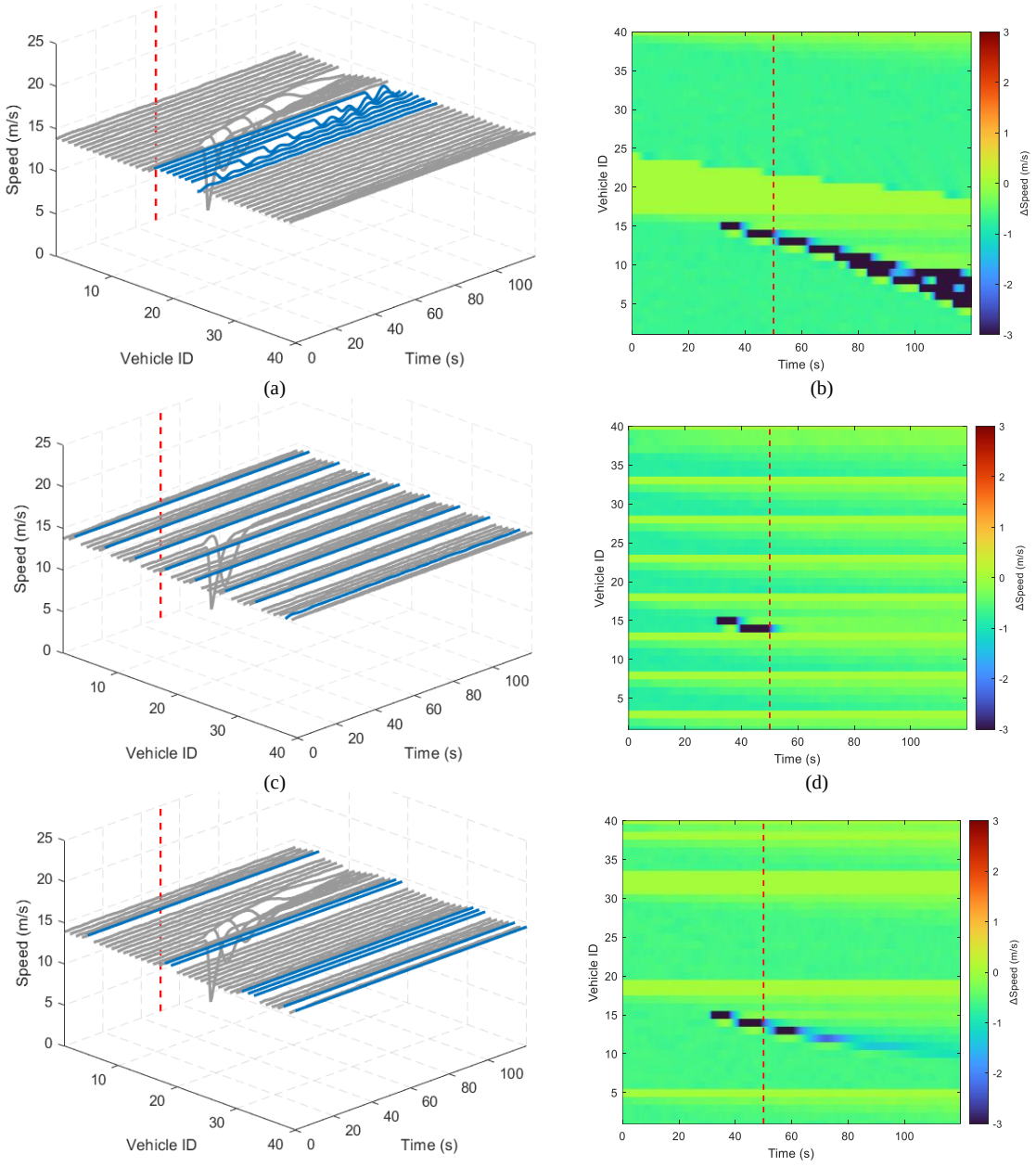

Fig. 5. Velocity trajectories and speed-residual plots under the three CAV spatial distribution strategies: (a) platoon distribution speed trajectory and (b) speed-residual plots; (c) uniform distribution speed trajectory and (d) speed-residual plots; (e) random distribution speed trajectory and (f) speed-residual plots.

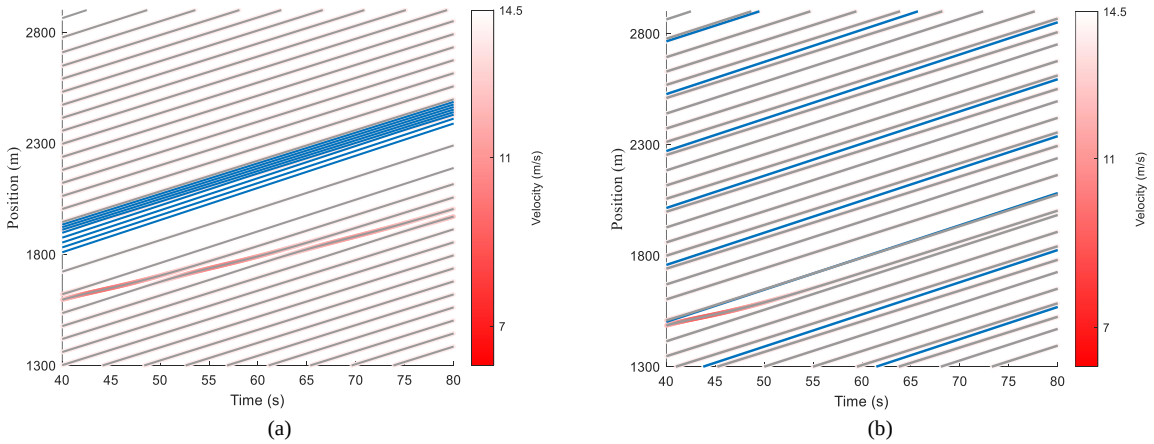

Fig. 6. Spatiotemporal trajectory plots for the (a) platoon distribution and the (b) uniform distribution.

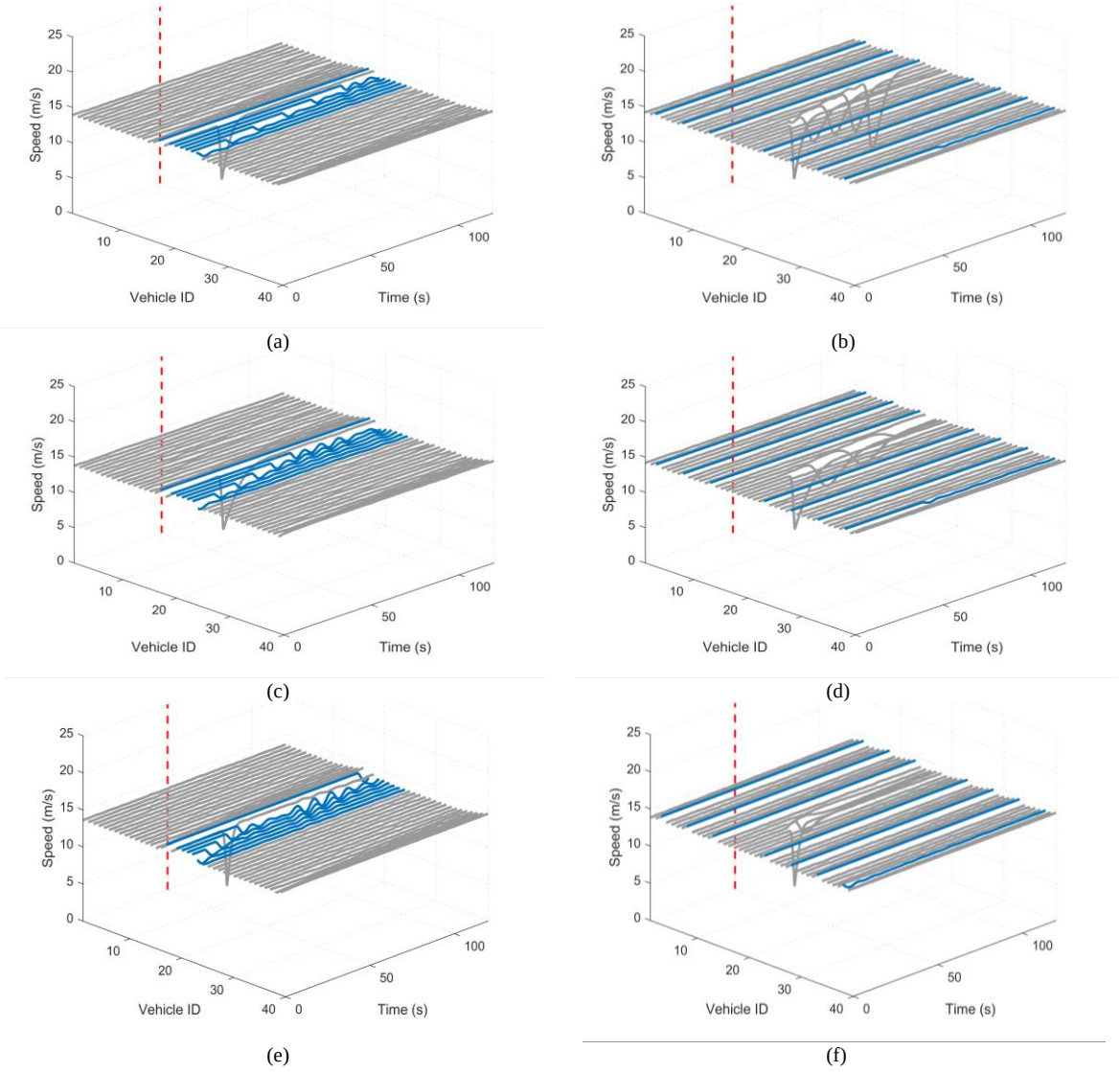

Fig. 7. Velocity trajectories under disturbance for the platoon distribution and uniform distribution CAV layouts at different HDV stability levels: (a) velocity trajectories for platoon and (b) uniform CAV distributions under strong HDV string-stability; (c) Velocity trajectories for platoon and (d) uniform CAV distributions under weak HDV string-stability; (e) Velocity trajectories for platoon and (f) uniform CAV distributions under HDV instability.

C. *Stability Evaluation Metrics*

The following is the definition of the L2 energy. Given the speed deviation curve of vehicle i over the time interval [0, T]

$$e_i(t) = v_i(t) - v_{\text{ref}}, \tag{32}$$

where v_{ref} is the equilibrium speed, the L2 energy of the entire platoon over the time interval [0, T] is defined as

$$L_2 = \int_0^T \sum_{i=1}^{N} \left[e_i(t) \right]^2 \mathrm{d}t = \sum_{i=1}^{N} \int_0^T e_i^2(t) \mathrm{d}t. \tag{33}$$

Treat the linearised dynamics of the mixed platoon (or local linear model) as a multi-input multi-output system:

$$\dot{x}(t) = Ax(t) + Bu(t), \tag{34}$$

$$y(t) = Cx(t), \tag{35}$$

where $u(t)$ is the disturbance input (the emergency-braking action of vehicle i), $y(t)$ is the output vector (the speed deviations of all vehicles), and $x(t)$ denotes the system state. The H2 norm of the system is defined as the energy of the impulse response from $u(t)$ to $y(t)$ as

$$\left\| G(s) \right\|_2 = \sqrt{\frac{1}{2\pi} \int_{-\infty}^{\infty} \operatorname{trace}\left[G_n(\omega) G_n^*(\omega) \right] \mathrm{d}\omega}. \tag{36}$$

When these three performance metrics are compared across various disturbance locations, the above observations are confirmed. In most cases (Fig. 8)., the uniform distribution outperforms the platoon distribution, with exceptions occurring only when the perturbation originates immediately in front of the platoon's lead vehicle. This finding indicates that, while platooning can effectively dissipate disturbances introduced directly ahead of the platoon, at lower penetration rates disturbances are more likely to occur elsewhere. Under such conditions, alternative deployment strategies, such as uniform CAV distribution, offer greater potential to reduce undesirable instabilities and enhance overall traffic flow efficiency.

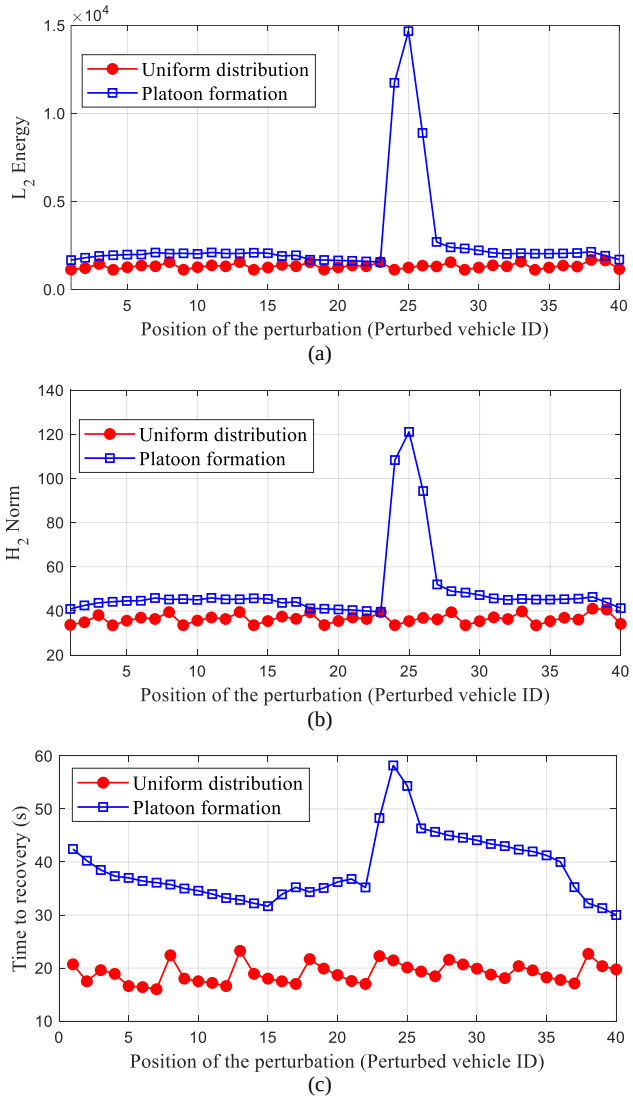

Fig. 8. Variation of energy, norm, and recovery time for platoon and uniform CAV distributions under different disturbance locations: (a) L_2 energy for different disturbance locations; (b) H_2 norm for different disturbance locations; (c) Recovery time for different disturbance locations.

V. CONCLUSIONS

This study investigates how the spatial distribution of connected and automated vehicles (CAVs) affects the performance of mixed traffic flow. We first established the underlying car-following models and then conducted perturbation experiments and numerical simulations to characterise mixed flow dynamics. The three-dimensional velocity surfaces demonstrate that the introduction of CAVs can, to varying degrees, attenuate stop-and-go wave propagation and enhance throughput. Based on a closed, single-lane ring-road configuration, our qualitative and quantitative analyses lead to the following conclusions: platoon distribution and uniform distribution are the two primary spatial deployment strategies. When human-driven vehicles (HDVs) exhibit poor string stability, platooning may be the least effective approach for disturbance mitigation, and, indeed, its relative performance may range from optimal to worst depending on HDV car-following behaviour and the traffic flow equilibrium state. It should be noted that this study is confined to high-density, oscillatory traffic under low-speed conditions (<15 m/s). Future work should extend the simulation framework to encompass a broader spectrum of traffic scenarios and conduct large-scale studies - using high-fidelity platforms such as SUMO or VISSIM - to evaluate the potential of different CAV deployment patterns in more realistic mixed-traffic environments, including lane change manoeuvres and other common driving behaviours.

CONFLICTS OF INTEREST

The authors declare that they have no conflicts of interest.

REFERENCES

[1] A. Eskandarian, C. Wu, and C. Sun, "Research advances and challenges of autonomous and connected ground vehicles", *IEEE Transactions on Intelligent Transportation Systems*, vol. 22, no. 2, pp. 683–711, 2021. DOI: 10.1109/TITS.2019.2958352.

[2] Y. Sugiyama *et al.*, "Traffic jams without bottlenecks—Experimental evidence for the physical mechanism of the formation of a jam", *New Journal of Physics*, vol. 10, art. no. 033001, pp. 1–7, 2008. DOI: 10.1088/1367-2630/10/3/033001.

[3] J. Dong, J. Wang, L. Chen, Z. Gao, and D. Luo, "Effect of adaptive cruise control on mixed traffic flow: A comparison of constant time gap policy with variable time gap policy", *Journal of Advanced Transportation*, vol. 2021, art. ID 3745989, pp. 1–13, 2021. DOI: 10.1155/2021/3745989.

[4] L. Xiao, M. Wang, W. Schakel, and B. van Arem, "Unravelling effects of cooperative adaptive cruise control deactivation on traffic flow characteristics at merging bottlenecks", *Transportation Research Part C: Emerging Technologies*, vol. 96, pp. 380–397, 2018. DOI: 10.1016/j.trc.2018.10.008.

[5] Y. Zhou, S. Ahn, M. Wang, and S. P. Hoogendoorn, "Stabilizing mixed vehicular platoons with connected automated vehicles: An H-infinity approach", *Transportation Research Part B: Methodological*, vol. 132, pp. 152–170, 2020. DOI: 10.1016/j.trb.2019.06.005.

[6] H. Gao, Y. Cen, B. Liu, X. Song, H. Liu, and J. Liu, "A collaborative merging method for connected and automated vehicle platoons in a freeway merging area with considerations for safety and efficiency", *Sensors*, vol. 23, no. 9, p. 4401, 2023. DOI: 10.3390/s23094401.

[7] Y. Li *et al*., "An improved eco-driving strategy for mixed platoons of autonomous and human-driven vehicles", *Physica A: Statistical Mechanics and its Applications*, vol. 641, art. no. 129733, 2024. DOI: 10.1016/j.physa.2024.129733.

[8] Y. Zhou, M. Wang, and S. Ahn, "Distributed model predictive control approach for cooperative car-following with guaranteed local and string stability", *Transportation Research Part B: Methodological*, vol. 128, pp. 69–86, 2019. DOI: 10.1016/j.trb.2019.07.001.

[9] R. Kianfar *et al*., "Design and experimental validation of a cooperative driving system in the grand cooperative driving challenge", *IEEE Transactions on Intelligent Transportation Systems*, vol. 13, no. 3, pp. 994–1007, 2012. DOI: 10.1109/TITS.2012.2186513.

[10] T. Robinson, E. Chan, and E. Coelingh, "Operating platoons on public motorways: An introduction to the SARTRE platooning programme", in *Proc. of the 17th World Congress on Intelligent Transportation Systems*, 2010, p. 12.

[11] S. Tsugawa, S. Kato, and K. Aoki, "An automated truck platoon for energy saving", in *Proc. of 2011 IEEE/RSJ International Conference on Intelligent Robots and Systems*, 2011, pp. 4109–4114. DOI: 10.1109/IROS.2011.6094549.

[12] W. Du, Z. Huang, S. Li, and J. Zhang, "Fundamental diagram and stability analysis of mixed traffic flow considering platoon intensity and multiclass time delay", *Physica A: Statistical Mechanics and its Applications*, vol. 675, art. no. 130847, 2025. DOI: 10.1016/j.physa.2025.130847.

[13] S. Zheng *et al*., "Oscillation growth in mixed traffic flow of human driven vehicles and automated vehicles: Experimental study and simulation", in *Traffic and Granular Flow '22. TGF 2022. Lecture Notes in Civil Engineering*, vol. 443. Springer, Singapore, 2024. DOI: 10.1007/978-981-99-7976-9_33.

[14] W. Ren, X. Zhao, H. Li, and Q. Fu, "Traffic flow impact of mixed heterogeneous platoons on highways: An approach combining driving simulation and microscopic traffic simulation", *Physica A: Statistical Mechanics and its Applications*, vol. 643, art. 129803, 2024. DOI: 10.1016/j.physa.2024.129803.

[15] S. Maiti, S. Winter, L. Kulik, and S. Sarkar, "Ad-hoc platoon formation and dissolution strategies for multi-lane highways", *Journal of Intelligent Transportation Systems*, vol. 27, pp. 161–173, 2023. DOI: 10.1080/15472450.2021.1993212.

[16] K. Li, J. Wang, and Y. Zheng, "Cooperative formation of autonomous vehicles in mixed traffic flow: Beyond platooning", *IEEE Transactions on Intelligent Transportation Systems*, vol. 23, no. 9, pp. 15951–15966, 2022. DOI: 10.1109/TITS.2022.3146612.